Annual Project Summary

High-resolution 3-D velocity model for Northridge-Los Angeles basin area from tomographic inversion of local arrival time data

External Grant Award Number: 03HQGR0064

Jose Pujol
Center for Earthquake Research and Information
The University of Memphis, Memphis, TN 38152
Phone: (901) 678-4827 Fax: (901) 678-4734 Email: pujol@ceri.memphis.edu

Non-technical summary

We determined a high-resolution 3-D velocity model for the San Fernando basin using arrival times from aftershocks of the Northridge and San Fernando earthquakes. Our model shows an overall good agreement with the Southern California Earthquake Center (SCEC) model, but our results indicate that parts of the basin are actually deeper than what the SCEC model predicts. Most of the Northridge aftershocks occurred within the basin, while those in the basement occurred in the vicinity of the rupture plane. The fault planes of the Northridge and San Fernando earthquakes do not truncate each other.

Results

Our research targeted the Los Angeles area, but we concentrated on the San Fernando basin because of the the large amount of data available and the relatively high station coverage. In addition, for the San Fernando basin we proceeded in two stages. In the first one we used arrival times from aftershocks of the Northridge earthquake recorded in 1994, while in the second stage all the aftershocks through 2000 were used. In both cases aftershock data from the San Fernando earthquake were used. The first stage has been completed and our results are essentially final and will be presented here. The second stage has also been completed and now we are checking our results, which basically confirm the previous ones.

In the first stage we used 4177 events in the Northridge mainshock-aftershock sequence recorded by 63 permanent and portable stations and 799 events from the San Fernando aftershock sequence recorded by 20 portable stations. The iterative tomographic inversion package of Benz (Benz et al., 1996) was used. This package includes software for the computation of travel times designed to handle sharp velocity discontinuities without approximations (Podvin and Lecomte, 1991), and the high resolution of our results derives from the use of this software. The velocity model was parameterized by $2 \times 2 \times 2$ km blocks and covers an 80 km x 80 km area. To assess the effect of the initial velocity model in the inversion results, two of them were used. One was a coarse 3-D velocity model determined using the same inversion software applied to a 300 km $\times$ 300 km area with $5 \times 5 \times 3$ km blocks (Shen, 1999). The second model was the 3-D SCEC model (Magistrale et al., 2000). The results for the two models are different in the details only; the main features are similar.

Using the coarse initial velocity model, the initial and final averaged RMS arrival-time residuals are 0.24 s 0.07 s (iteration 14), respectively. The final event locations are shifted 1.5 km to the east, 0.4 km to the north, and 0.6 km up, on average, with respect to the initial single-event locations, in addition to becoming more clustered, in agreement with our earlier results (Pujol, 1996).

Our main results are described in the captions to the following figures, and can be summarized as follows. A narrow and well-defined 10 km wide lineation of Northridge aftershocks occurred in the basement between about 10 and 20 km depth and define the fault that slipped during the mainshock. This fault plane inferred from the seismicity is in good qualitative agreement with the geodetic fault plane determined by Hudnut et al. (1996). Horizontal velocity slices show that the Northridge earthquake occurred within a narrow basement wedge, which may have controlled the size of the earthquake. A strong cluster of aftershocks at about 10 km depth roughly along the fault plane may be associated with the fact that this is the area where the main shock rupture reached the bottom of the basin. Other authors interpreted this cluster as an indication of deformation in an anticlinal fold. Most of the aftershocks of the Northridge earthquake occurred within the basin with a large concentration of them to the east of the eastern boundary of the mainshock fault plane. The latter events also dip to the southwest, most of them are shallower than 12-13 km and form a band of seismicity 3 to 4 km wide within and near the edge of the basin. These results are confirmed by the inversion of the larger data set of arrival times from Northridge aftershocks recorded through 2000. These events are not on the mainshock fault plane and taking this fact into account shows that the San Fernando and the Northridge mainshocks occurred on en-echelon conjugate faults, which means that the San Fernando fault did not truncate the Northridge fault, as commonly stated. On the other hand, an 8 km wide almost N-S cross section of the Northridge aftershocks east of the mainshock and aftershocks of the San Fernando earthquake shows that the seismicity takes place around a high-velocity basement block. We interpret this result as an indication that this basement high remained elevated during the opening of the basin, with the observed seismicity occurring in the weaker sediments around its flanks.

Data availability

The velocity model and event locations are in binary and ASCII formats, respectively, and are available from J. Pujol (phone: 901-678-4827; email: pujol@ceri.memphis.edu).

References

Benz, H., B. Chouet, P. Dawson, J. Lahr, R. Page, and J. Hole (1996). Three-dimensional P and S wave velocity structure of Redoubt volcano, Alaska, *J. Geophys. Res.* **101**, 8111-8128.

Hudnut, K., and ten others (1996). Co-seismic displacements of the 1994 Northridge, California, earthquake, *Bull. Seism. Soc. Am.* **86**, S19-S36.

Langenheim, V., A. Griscom, R. Jachens, and T. Hildenbrand (2000). Preliminary potential-field constraints on the geometry of the San Fernando basin, southern California, *U.S.G.S. Open-file Report* **00-219**.

Magistrale, H., S. Day, R. Clayton, and R. Graves (2000). The SCEC southern California reference three-dimensional seismic velocity model version 2, *Bull. Seism. Soc. Am.* **90**, S65-S76.

Podvin, P., and I. Lecomte (1991). Finite difference computation of traveltimes in very contrasted velocity models: A massively parallel approach and its associated tools, *Geophys. J. Int.* **105**, 271-284.

Pujol, J. An integrated 3D velocity inversion – joint hypocentral determination analysis of events in the Northridge area, *Bull. Seism. Soc. Am.* **86**, S138-155.

Shen, P. (1999). Simultaneous travel time inversion for 3D velocity model and earthquake locations: application to the Northridge, California, 1994 mainshock-aftershock sequence, M.S. thesis, The University of Memphis.

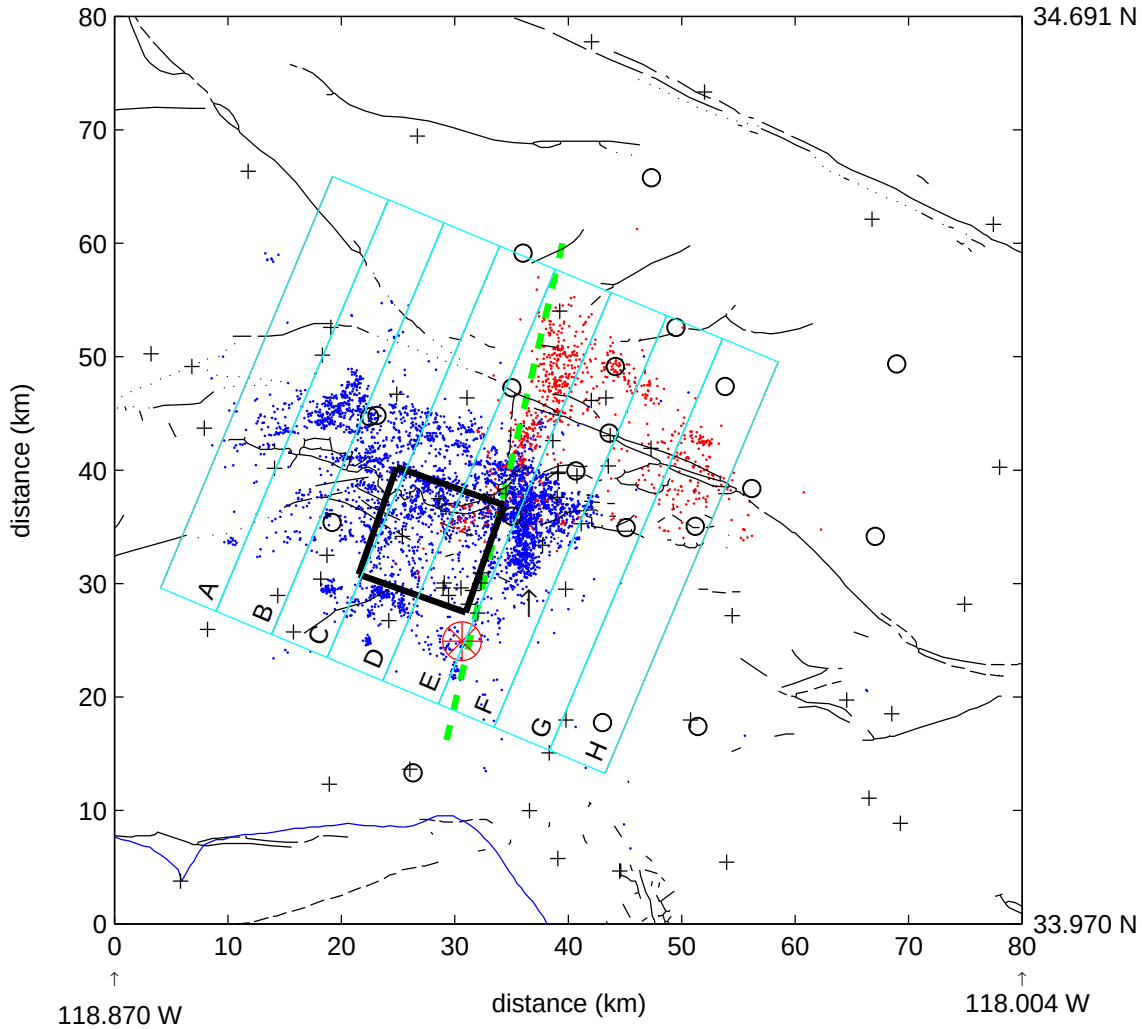

Figure 1. Area for which a 3-D velocity model has been determined. Blue and red dots indicate aftershocks of the Northridge and San Fernando earthquakes, recorded during 1994 and February-April 1971, respectively. The circled asterisk indicates the Northridge main shock. The locations were determined as part of the velocity inversion - earthquake location process. Circles and pluses denote the stations used to locate the San Fernando and Northridge events. The bold rectangle is the projection of the fault plane determined by Hudnut et al. (1996) assuming uniform slip. The events in the labeled boxes are shown in cross section in Fig. 3. Most of the San Fernando events are to the east of the green dashed line while the Northridge main shock rupture occurred to the west of that line. The prominent band of Northridge seismicity in a roughly N-S direction (identified by the arrow in box F) did not occur within the area that ruptured during the main shock. These events are also shown in cross section in Fig. 6.

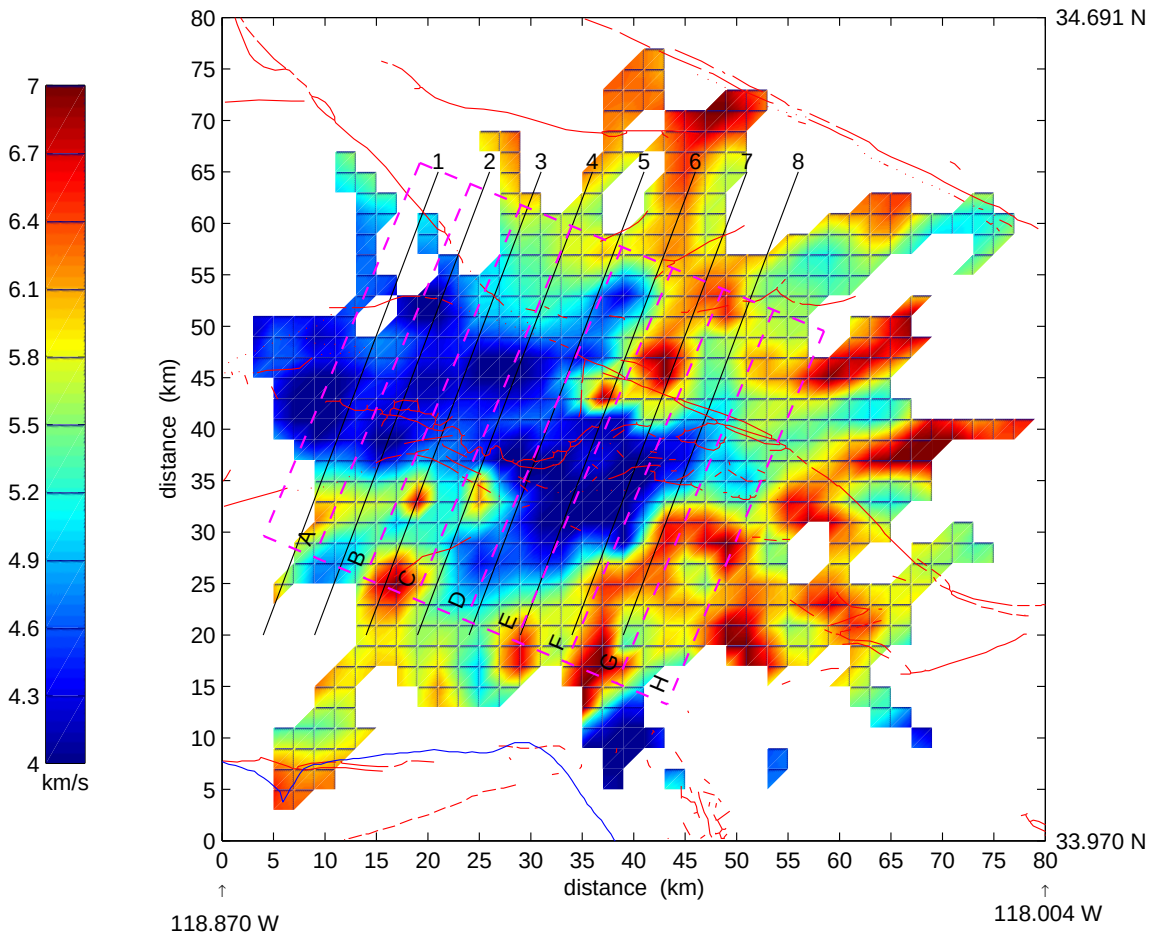

Figure 2. Map view of the upper layer of the 3-D velocity model determined by tomographic inversion. The ragged appearance is due to the fact that only blocks covered by more than five rays are shown. The initial velocity model was derived from a coarser 3-D model generated for a wider area. The central and southern low-velocity areas correspond to the San Fernando and Ventura basins and to the Los Angeles basin, respectively. Velocity cross sections are shown in Figure 3. The labeled boxes coincide with those in Fig. 1.

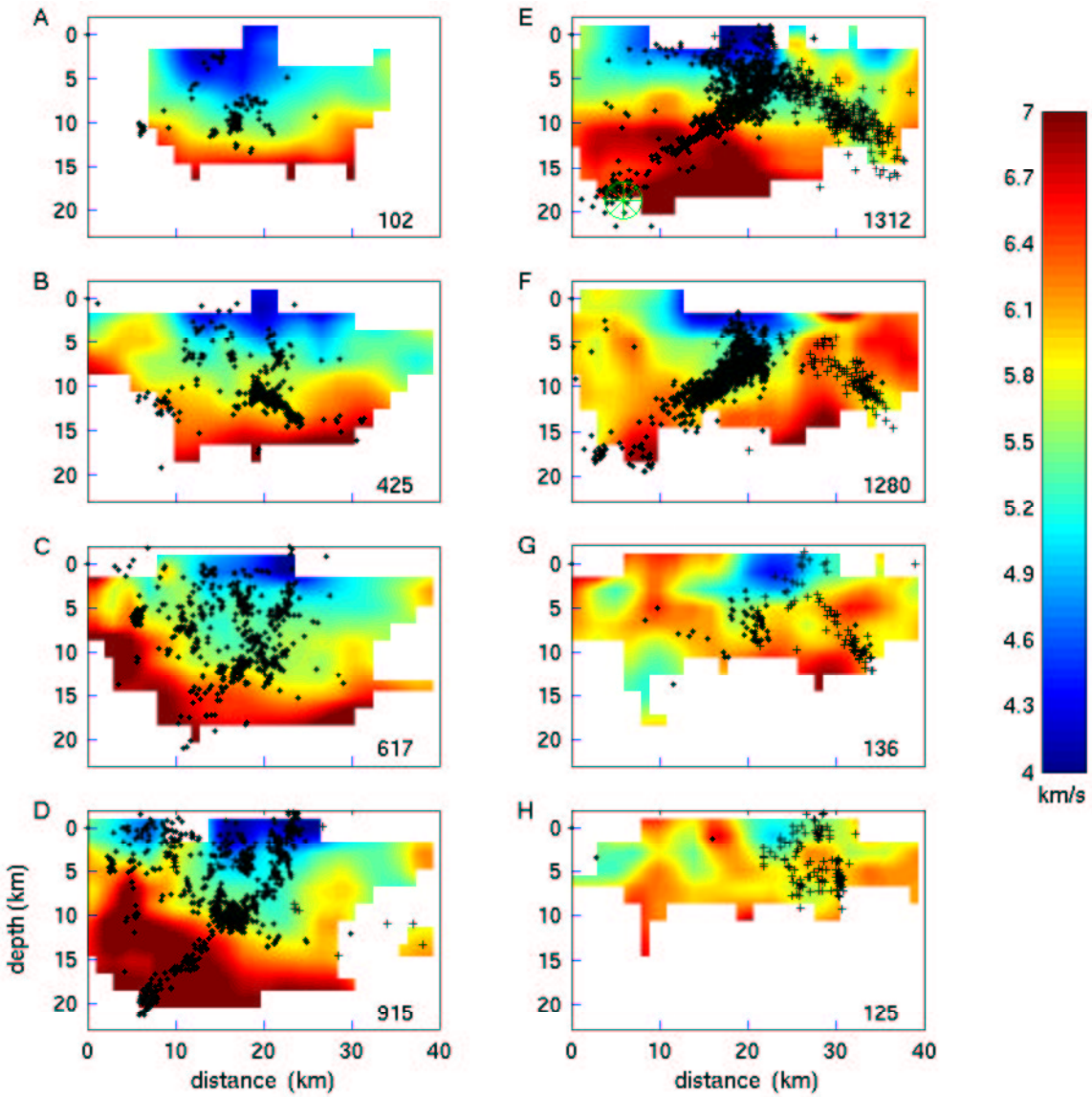

Figure 3. Depth cross sections for the velocity model and the events in the labeled boxes in Figs. 1 and 2. The width of the cross sections is 5.3 km. The letters are on the southern ends of the cross sections. Black asterisks and pluses indicate Northridge and San Fernando aftershocks and the green asterisk in cross section E indicates the Northridge main shock. The number in the right lower corner of each cross section denotes the number of events. Only the velocity blocks covered by more than five rays are shown. Note the correlation between seismicity and velocity. The events between about 10 and 20 km in D and E are within high-velocity, basement rocks, and form narrow and well-defined lineations. These events span about 10 km horizontally and basically define the width of the fault that slipped during the main shock. The strong concentration of events at about 10 km depth and 15 km distance in D may be associated with the fact that this is the area where the main shock rupture reached the bottom of the basin. Langenheim et al. (2000) made a similar comment based on the modeling of gravity data. The Northridge aftershocks in F correspond mostly to those indicated by an arrow in Fig. 1. Most of these events are shallower than 15 km and form a band of seismicity 3 to 4 km wide within and near the edge of the basin. Most of the seismicity in A, B, and C occurs within the basin. The events in B between about 10 and 15 km depth around a distance of 20 km are likely to correspond to the Santa Susana fault.

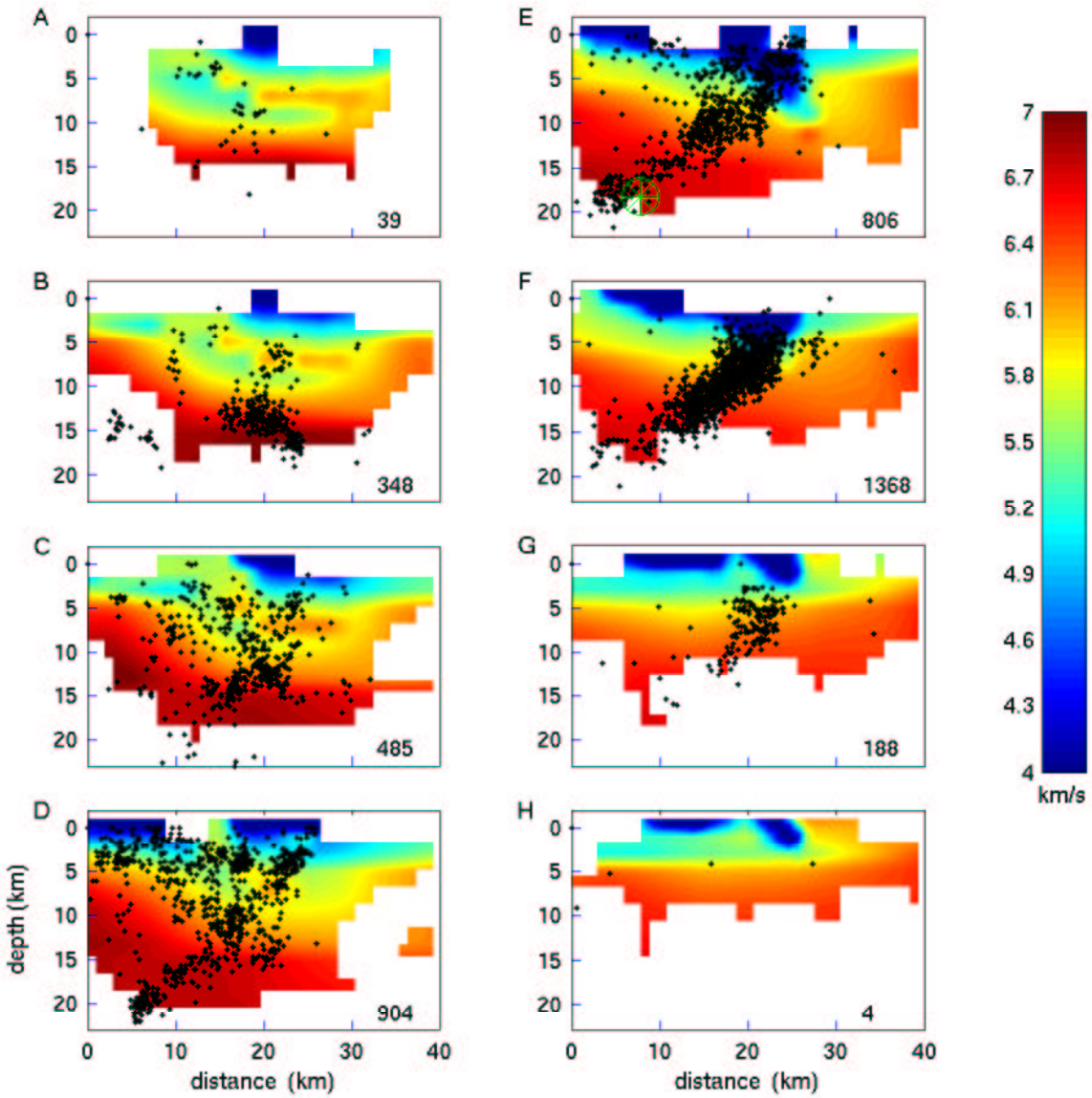

Figure 4. Similar to Fig. 3 for the SCEC 3-D velocity model and SCEC single-event locations.

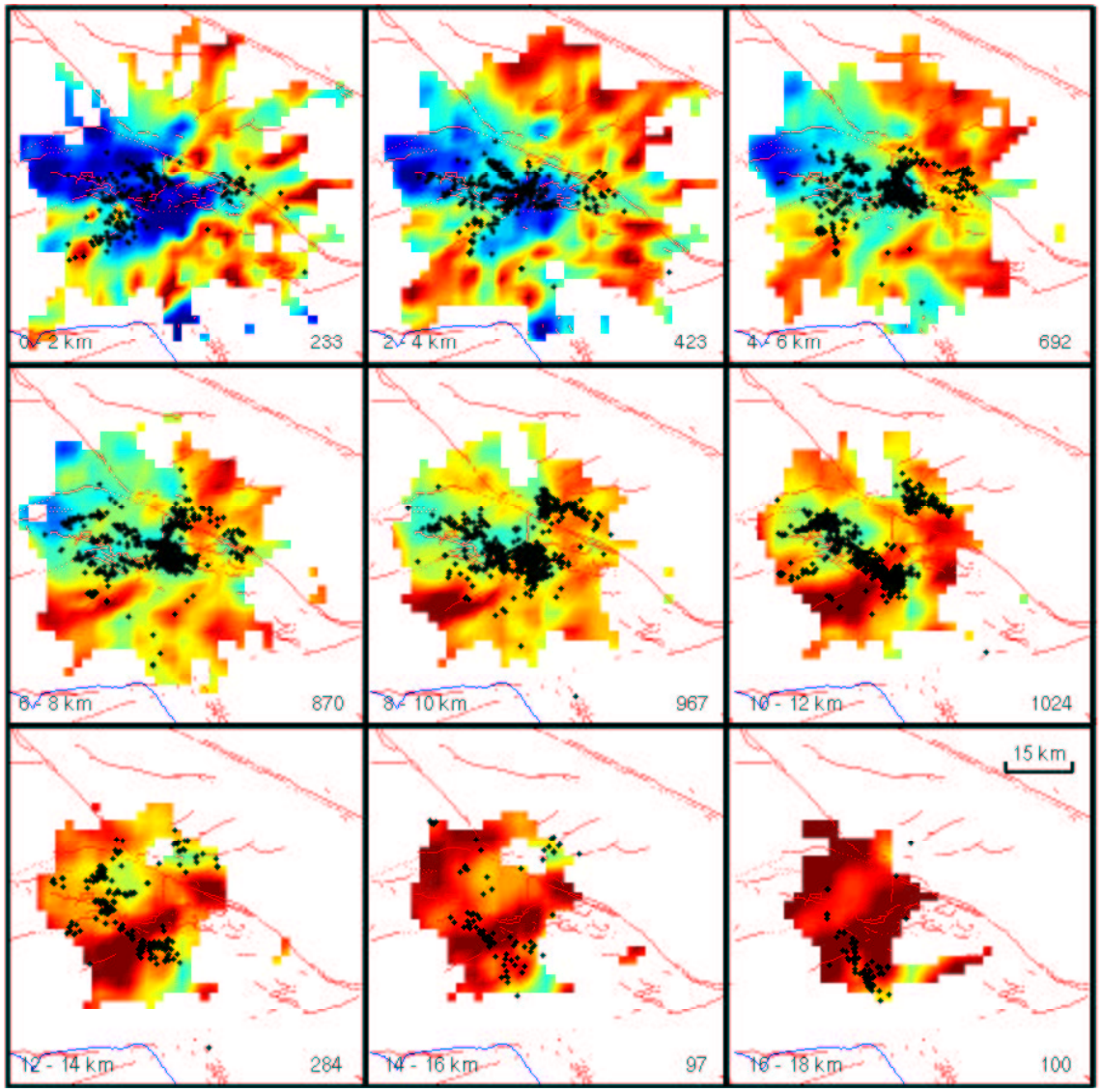

Figure 5. Map view of the velocity model as a function of depth. The numbers on the left lower corners indicate the depth range. Also shown are the inversion locations. The numbers on the right lower corners indicate the number of events. Note below 10 km depth the events that occur within or close to a high velocity wedge.

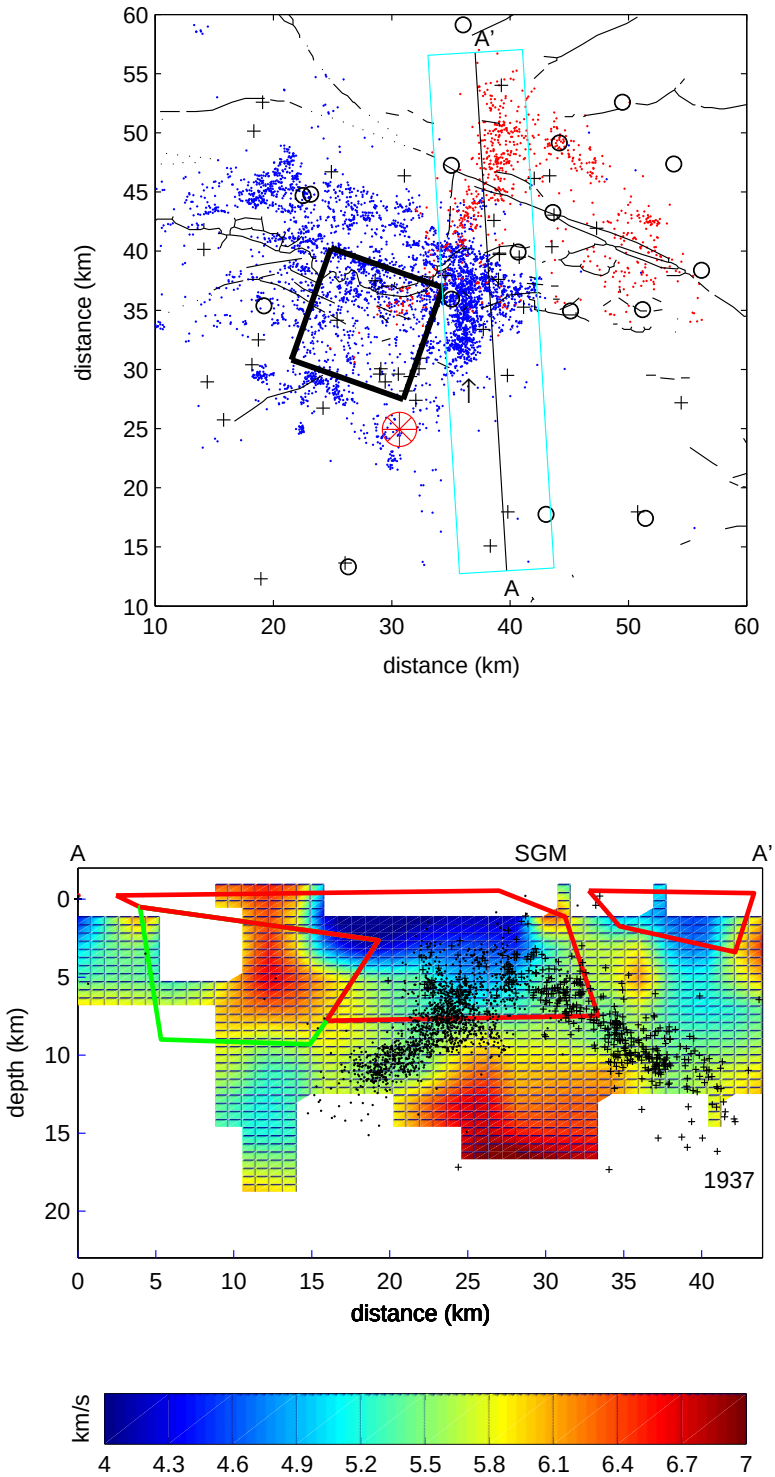

Figure 6. TOP: Similar to Fig. 1. The events in the blue box are shown in cross section below. BOTTOM: Depth cross sections for the velocity model and the events in the box above and model (simplified) used by Langenheim et al. (2000) to match observed gravity profiles. The red lines bound materials with densities ranging between 2.00 and 2.55 g/cm^3. The area bounded by red and green lines corresponds to low-density basement (2.65 g/cm^3). Elsewhere in the figure the density is 2.71 g/cm^3. Note that the velocity model correctly predicts high velocities in the San Gabriel Mountains area (indicated by SGM). Also note that the Northridge and San Fernando aftershocks are underlain by a wedge of basement, with the seismicity taking place where velocities are lower. We interpret this result as an indication that this basement wedge remained elevated during the opening of the basin, with the observed seismicity occurring in the weaker sediments around its flanks.